International Journal of Applied Power Engineering (IJAPE)
Vol. 15, No. 3, September 2026, pp. 1439~1457
ISSN: 2252-8792, DOI: 10.11591/ijape.v15.i3.pp1439-1457

Voltage stability analysis of power transmission systems using multi-index framework of hybrid whale and particle swarm optimization technique

Titus Terwase Akor[1], Theophilus Chukwudolue Madueme[2], Chibuike Peter Ohanu[1,2], Tole Sutikno[3,4]
[1]Africa Centre of Excellence for Sustainable Power and Energy Development (ACE-SPED), University of Nigeria, Nsukka, Nigeria
[2]Department of Electrical Engineering, Faculty of Engineering, University of Nigeria, Nsukka, Nigeria
[3]Department of Electrical Engineering, Faculty of Industrial Technology, Universitas Ahmad Dahlan, Yogyakarta, Indonesia
[4]Embedded System and Power Electronics Research Group, Yogyakarta, Indonesia

Article Info

Article history:

Received Dec 8, 2025
Revised Jul 1, 2026
Accepted Aug 15, 2026

Keywords:

Analysis
Multi-index framework
Optimization
Transmission system
Voltage stability

ABSTRACT

The persistent increase in grid collapse has necessitated the need for robust solutions for stability. Hybrid whale and particle swarm optimization (WAPSO) algorithm integrated with multi-index stability indices (MIS) has been applied to enhance voltage stability in this paper. The method is tested on the Nigeria 48-bus, 330 kV transmission system and simulated in MATPOWER embedded in MATLAB. The WAPSO algorithm is optimized with parameters $w = 0.4$, $c_1 = 1.4$ and $c_2 = 1.5$. The outcome achieved 98.84% reduction in mean MIS from 0.3959 to 0.0048 and a robustness index of 0.0051. This depicts low variability of 0.057 and 100% success rate across five dynamic scenarios explored such as gradual load growth with 98.79%, sudden spikes achieved 98.84%, cyclic fluctuations at 98.67%, renewable uncertainty at 98.74%, and N-1 contingencies at 98.84% improvement, respectively. Critical lines, 34-35 and 24-33 exhibit more than 99% MIS improvement, while weak lines, 21-22 and 24-40 achieved 85–87% enhancement, indicating areas for further reinforcement. The LSI and FVSI are reduced to 0.0048 and 0.1477 showing 56.79% improvement respectively as against the 38.9% MIS improvement obtained with the PSO-GA. This demonstrates WAPSO as a highly robust and adaptable technique offering a scalable solution for enhancing grid reliability under dynamic conditions.

Corresponding Author:

Chibuike Peter Ohanu
Africa Centre of Excellence for Sustainable Power and Energy Development (ACE-SPED)
University of Nigeria
Nsukka, Nigeria
Email: chibuike.ohanu@unn.edu.ng

1. INTRODUCTION

The evaluation of voltage stability is among the most interesting studies in the domain of power systems. The concept of voltage stability describes the capacity of a power system to sustain constant voltages at each bus after experiencing a disruption from a certain initial operating condition. The ability of power transmission system to maintain balance between load demand and supply is a criterion for stability assessment. One possible indicator of this instability is the gradual increment or reduction in voltages of some buses in the network as presented in [1]. Voltage instability can result in cascade outages, loss of generator synchronism, or localized load loss. It can also cause transmission lines and other network components to trip due to safety mechanisms, as stated in [2]. In order to plan for and predict voltage collapse, engineers rely heavily on voltage stability analysis as enumerated in [3]. Various strategies can be applied to tackle voltage instability and contingencies on the power transmission system. Stability is a critical factor in ensuring the reliability of a power system during outages, as emphasized in [4]. Power system stability remains a key research area in electrical engineering, with voltage stability analysis as the main indicator. Given the increasing demand for electricity, maintaining a reliable power infrastructure is essential. The Nigerian electrical grid faces multiple challenges, including sabotage, long transmission lines, inadequate wheeling power, frequent grid failures, vandalism, outdated infrastructure, fuel shortages, insufficient investment, and weak distribution network.

Several researchers have discussed instability and contingencies in power transmission network however, there are many shortfalls despite numerous solutions. For instance, authors in [5] reported 573 partial and total grid failures in Nigeria between 2000 and 2022. Additionally, the work in [6] documented three failures in 2023, while the study in [7] recorded five collapses in 2024, consisting of one partial failure and four total breakdowns. Data from the transmission company of nigeria (TCN), an independent system operator [8] further revealed seven system collapses, bringing the total failures in 2024 to twelve and the cumulative failures between 2000 and 2024 to 588. Two system collapse events occurred in 2025 and an additional two in January 2026, resulting in a total of 592 recorded incidents over the past 27 years as reported by Nigerian Independent System Operator. The frequent grid failures are due to multiple causes; including generation losses, transmission line and transformer overloads. Issues like high voltages, cascading faults, high-frequency deviation, a weak grid network, infrastructure limitations, protective device malfunctions, natural disasters such as flooding, and intentional sabotage are highlighted in [6], [8]–[11]. If we want to achieve long-term economic advancement and energy security, substantial investments in power infrastructure are necessary to enhance grid stability and reliability. Table 1 presents a 25-year summary of grid failures with total blackouts surpassing partial breakdowns, underscoring the broader economic implications of the country's energy crisis [5]–[9]. The recurring grid collapse impose significant economic costs. The World Bank estimates that unreliable electricity supply reduces Nigeria's GDP by 5% to 7% annually, this is equivalent to about 7–10 trillion naira (US$25 billion) loss in productivity and investment [12]. Similarly, the African Development Bank (ADP) reported that the country loses roughly US$29 billion each year or about 5.8% of GDP due to inadequate and unstable power supply [13]. Each blackout can cost the economy over US$100 million per day; disrupting manufacturing, telecommunications, and financial services. These impacts reveal the urgency of strengthening voltage stability to enhance both energy reliability and national economic resilience.

Table 1. Nigerian grid collapse for the period of year 2000–2026

S/N	Year	Total blackout	Partial blackout	Total	S/n	Year	Total blackout	Partial blackout	Total
1	2000	5	6	11	15	2014	9	4	13
2	2001	14	5	19	16	2015	6	4	10
3	2002	9	32	41	17	2016	22	6	28
4	2003	14	39	53	18	2017	15	9	24
5	2004	22	30	52	19	2018	12	1	13
6	2005	21	15	36	20	2019	7	4	10
7	2006	20	10	30	21	2020	3	1	4
8	2007	18	8	26	22	2021	2	2	4
9	2008	26	16	42	23	2022	6	2	8
10	2009	19	20	39	24	2023	2	1	3
11	2010	22	20	42	25	2024	10	2	12
12	2011	13	6	19	26	2025	2	0	2
13	2012	16	8	24	27	2026	2	0	2
14	2013	22	2	24		Total	339	253	592

2. SUMMARY OF REVIEWED LITERATURE

The study in [14] reported the occurrences of voltage collapse between 2000 and 2017; however, it did not perform any analytical investigation to propose solutions to the identified problems. While study in [15] illustrated the use of reactive power compensation to address voltage instability but failed to address dynamic disturbance variation. The report in [16] evaluated a modern voltage stability index for predicting voltage collapse and identifying weak buses and critical lines. This proves that there are effective indices but the results lacks an optimization techniques integration. To enhance power quality [17], [18] applied a glow-worm swarm optimizer, yet further optimization and multi-index approaches remain unexplored. Study in [19] proposed a relay-based local index addressing both voltage stability and line protection, effectively distinguishing between stable and unstable cases during disturbances. Researchers in [20] employed Modal/Eigenvalue analysis to assess Nigerian power system stability. Contrastly, [21] validated a quadratic approximation for load margin estimation, proposing power flow equation modifications to identify critical contingencies, though rankings remained imprecise. Article in [22] improved distribution network voltage stability by tuning a voltage stability index using the fast voltage stability indicator and simulated annealing optimization. Badrudeen *et al.* [23] introduced a novel voltage stability pointer (NVSP) trained with SVM and the medium Gaussian kernel classification toolbox (mGkCT) in MATLAB, effectively distinguishing stable and unstable lines. Studies in [24], [25] analyzed voltage stability indices to identify weak buses and employed PSO to mitigate power losses. However, the studies in [26], [27] relied on a single stability index, despite multi-index approaches offering greater accuracy, sensitivity, and adaptability.

2.1. Statement of problems and research contributions

The problems identified in this research after an extensive literature review indicate the following:

- Traditional static stability indices like line stability index (LSI), voltage stability index (VSI), loading margin (LM), FVSI often fail to account for real-time dynamic variations such as load growth, renewable energy fluctuations, N-1 contingencies, or sudden spikes.
- Conventional static optimization approaches such as deterministic MIS minimization exhibit over-optimism, producing solutions that degrade under disturbances and result in high variability (coefficient of variation, CV) in stability margins with limited adaptability. While hybrid metaheuristics like WAPSO is effective for multi-dimensional problems such as reactive power scaling across large networks, their effectiveness remains highly sensitive to parameter settings, particularly the inertia weight (w) and the cognitive/social coefficients (c_1, c_2).

The aforementioned problems formed the gaps in this paper, therefore, the main objective of this paper is to fill this gap by exploring voltage stability analysis through the integration of hybrid whale and particle swarm optimization algorithms with multi-index indices (fast voltage stability index and line stability index) to enhance network stability under real-time dynamic variations. This paper demonstrates that the proposed WAPSO approach delivers more reliable and scalable stability improvements than the PSO-GA method, owing to its superior robustness under dynamic conditions, reduced parameter sensitivity, and enhanced adaptability to real-time disturbances. The main contributions of this research are summarized as follows:

- Multiple scenario dynamic evaluation: This study developed five realistic operating scenarios including gradual growth, sudden demand spikes, cyclic load fluctuations, renewable uncertainty, and N-1 contingencies to test MIS performance under diverse conditions. By applying the WAPSO framework, the approach ensures resilience, achieving low variability (CV < 0.1) and high reliability (success rate > 90%).
- Comprehensive sensitivity analysis: The study systematically evaluated 27 parameter combinations of inertia weight (w) and cognitive/social coefficients (c_1, c_2) across 30 independent runs. A robustness index, defined as $\mu \times (1 + CV)$, is used to identify the most stable parameter set (lower values indicate stronger performance), thereby addressing the common gap in parameter tuning for metaheuristic algorithms.
- Re-optimization for adaptability: Simulates real-time corrective actions with a +30% Q_{re} disturbance and 20 re-optimization runs, ensuring <5% performance degradation. It demonstrates ~20–30% per-line MIS improvement through averaged results and interpretable visualizations (heatmaps, boxplots), addressing the lack of scenario-robust metrics.

2.2. Paper organization

This paper is organized as follows: Section 1 introduced the research topic and discussed the background at which the study is based. Section 2 presented an extensive literature review that helped in the indentifiction of gaps while section 3 presents the methodology, including the formulation of MIS, the definition of dynamic scenarios, the WAPSO algorithm, and IPFC modeling. Section 4 discussed the results, covering voltage profile improvements, MIS reductions, scenario-based performance, and comparative evaluation with PSO-GA. Finally, section 5 summarized all the findings and recommendation some future research directions.

3. MATERIALS AND METHODS

This research utilized the LSI and the fast voltage stability index (FVSI) as multiple stability indices. Each index was modeled individually before combining them into a composite stability measure. With reference to the line stability index suggested in [23], Figure 1 illustrates a schematic of a 2-bus network model. All parameters and variables are expressed in per-unit values. The problem formulation of LSI is further detailed in [28].

The parameters of Figure 1 are stated as follows: The line impedance is given by: $Z_L = R_L + jX_L$.

$$S_{re} = P_{re} + jQ_{re} = V_{re}I_{re}^* \tag{1}$$

Where,

$$I_{re}{}^{*} = \frac{\bar{V}}{\bar{Z_L}} = \frac{V_{se}\angle\delta_{se} - V_{re}\angle\delta_{re}}{Z_L\angle\theta} \tag{2}$$

Substituting in (2) into (1) we have (3).

$$S_{re} = V_{re}\angle\delta_{re}\left[\frac{V_{se}\angle\delta_{se} - V_{re}\angle\delta_{re}}{Z_L\angle\theta}\right] = \frac{|V_{se}||V_{re}|}{|Z_L|}\angle(\theta + \delta_{re} - \delta_{se}) - \frac{|V_{re}|^2}{|Z_L|}\angle\theta \tag{3}$$

After appropriate mathematical evaluation, we have (4).

$$1 - \frac{4XQ_{re}}{|V_{se}|^2 sin^2(\theta-\delta)} \geq 0 \tag{4}$$

Hence, the line stability index will be (5).

$$L_{hf} = \frac{4XQ_{re}}{|V_{se}|^2 sin^2(\theta-\delta),} \leq 1 \tag{5}$$

Formulation of the FVSI as proposed in [24]: Also considering Figure 1 and deriving from the Ohm's law in (6).

$$V = IZ \tag{6}$$

The actual current, I_{re} is expressed as (7).

$$I_{re} = \frac{V}{Z_L} \tag{7}$$

Using (1) and (2), we have (8).

$$I = \frac{V}{Z} = I_{re} = \frac{V_{se}\angle\delta_{se} - V_{re}\angle\delta_{re}}{Z_L\angle\theta} \tag{8}$$

And the receiving end current is given by (9).

$$I_{re} = \left(\frac{S_{re}}{V_{re}}\right)^{*} = \frac{P_{re} - jQ_{re}}{V_{re}\angle -\delta_{re}} \tag{9}$$

Substituting (8) into (9), we have (10).

$$\frac{V_{se}\angle\delta_{se} - V_{re}\angle\delta_{re}}{R + jX} = \frac{P_{re} - jQ_{re}}{V_{re}\angle -\delta_{re}} \tag{10}$$

By evaluating (11).

$$\frac{4XQ_{re}(Z^2)}{(V_{se}Rsin\,\delta - XV_{se}cos\,\delta)^2} \leq 1 \tag{11}$$

By assumption, if $\delta \to 0$, $sin\delta \to 0$ and $cos\delta \to 1$. Then, (12).

$$\frac{4XQ_{re}Z^2}{X^2 V_{se}{}^2} \leq 1 \tag{12}$$

Hence, the FVSI can be written as (13).

$$FVSI = \frac{4Q_{re}Z^2}{XV_{se}{}^2} \leq 1 \tag{13}$$

Bringing (5) and (13) together yields the multi-index stability indices (MIS) as shown in (14).

$$MIS = \frac{4Q_{re}}{|V_{se}|^2}\left[\frac{(|Z|)^2}{X}\sigma - \frac{X}{sin^2(\theta-\delta)}(\sigma - 1)\right] \leq 1 \quad \sigma = \begin{cases} -1, & \delta < \delta_c \\ 0, & \delta \geq \delta_c \end{cases} \tag{14}$$

Where δ is the modifier and δ_c is the threshold value. The (14) uses a switching function, σ, to determine voltage collapse proximity and compares each result to a threshold value. The function σ for switching is based on the insignificant fluctuation in angle, δ, which indicates a severely loaded power system grid. A considerable angle variation indicates high power flow or resistance. Stability is maintained when MIS is less than 1, but as it approaches 1, instability arises, resulting in voltage collapse as enumerated by [28]. A summary of key equations is shown in Table 2. The parameter σ characterizes the dominant instability mechanism as the system approaches voltage collapse. At low loads (σ≈0), instability is reactive-power-limited, whereas at high loads (σ≈1), it becomes angle-limited, amplifying power swings and risking synchronism loss. For the Nigerian grid, high σ values under peak demand highlight stressed operating conditions, underscoring the need for reinforcements such as FACTS devices to prevent cascading outages. The threshold angle (δ_c) defines the critical stability margin in the switching function σ(δ), marking the point where the MIS shifts between LSI- and FVSI-dominance. In transmission systems, active power transfer $P \approx (\frac{V_{se}V_{re}}{X})\sin(\delta)$ reaches its maximum, beyond which $\delta = 90^o$ stability deteriorates.

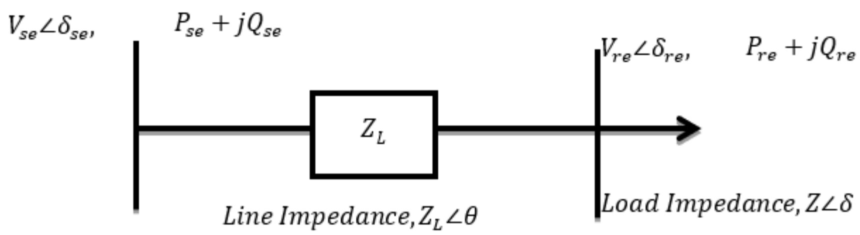

Figure 1. A transmission network model of a 2-bus system

Table 2. A summary of key equations

Index	Equation	Condition
LSI	$\frac{4XQ_{re}}{\lvert V_{se}\rvert^2 sin^2(\theta-\delta),} \leq 1$	-
FVSI	$\frac{4Q_{re}Z^2}{XV_{se}{}^2} \leq 1$	
MSI	$\frac{4Q_{re}}{\lvert V_{se}\rvert^2}\left[\frac{(\lvert Z\rvert)^2}{X}\sigma - \frac{X}{sin^2(\theta-\delta)}(\sigma-1)\right] \leq 1$	$\sigma = \begin{cases} -1, & \delta < \delta_c \\ 0, & \delta \geq \delta_c \end{cases}$, δ is the modifier and δ_c is the threshold value.

Practically, δ_c is set at or slightly below this value (typically 80°–85°) to provide a safety margin. It distinguishes secure operation ($\delta < \delta_c$) from stressed or emergency conditions ($\delta > \delta_c$), where small disturbances can trigger voltage collapse. It is important to note that the assumption δ→0 is introduced only as a mathematical simplification during the derivation of the FVSI formulation**.** In real transmission systems, the power angle difference is small but non-zero, typically ranging from 5° to 30° under normal operating conditions. Therefore, this approximation does not imply zero power transfer; rather, it simplifies the analytical expression while preserving the practical operating characteristics of the system.

Furthermore, although the maximum theoretical power transfer occurs at δ = 90º, practical transmission systems operate at significantly smaller power angles (typically 5°–40°) to maintain sufficient stability margins and prevent instability. Consequently, δ=90º represents only the theoretical steady-state stability limit, rather than an actual operating condition. Load flow analysis is applied to determine the steady-state solution of a particular power system. It provides an initial assessment of the power system, which is nonlinear due to the dynamic relationship between load, voltage magnitude, and circuit impedance. Since it is a non-linear problem, it has to be solved iteratively. The method has a better convergence rate than other methods of load flow solution as stated in [25]. The load flow formulation is given by (15) and (16).

$$P_h = \sum_{\substack{f=1 \\ f\neq h}}^{n} \lvert V_h\rvert \lvert V_f\rvert \lvert Y_{hf}\rvert cos(\theta_{hf} - \delta_h + \delta_f) \tag{15}$$

$$Q_h = -\sum_{\substack{f=1 \\ f\neq h}}^{n} \lvert V_h\rvert \lvert V_f\rvert \lvert Y_{hf}\rvert sin(\theta_{hf} - \delta_h + \delta_f) \tag{16}$$

The (15) and (16) form a set of non-linear algebraic equations. By applying a Taylor series expansion and neglecting higher-order terms, the system can be linearized, resulting in the Jacobian matrix formulation, which describes the interaction between voltage magnitude, voltage angle, and active and reactive power:

$$\begin{bmatrix} \Delta P \\ \Delta Q \end{bmatrix} = \begin{bmatrix} J_1 & J_2 \\ J_3 & J_4 \end{bmatrix} \begin{bmatrix} \Delta\delta \\ \Delta|V| \end{bmatrix} \tag{17}$$

where J_1, J_2, J_3, and J_4 are the submatrices of the Jacobian matrix. ΔP and ΔQ represent the mismatches between scheduled and calculated values of active and reactive power, respectively. $\Delta\delta$ and $\Delta|V|$ are the incremental corrections to the bus voltage angles and magnitudes. These mismatches at iteration k are expressed as: Thus,

$$\Delta P_h^k = P_h^{scheduled} - P_{h(calculated)}^k \tag{18}$$

$$\Delta Q_h^k = Q_h^{scheduled} - Q_{h(calculated)}^k \tag{19}$$

hence, the measured voltage magnitude and angle are given as (20) and (21).

$$\delta_h^{(k+1)} = \delta_h^{(k)} + \Delta\delta_h^{(k)} \tag{20}$$

$$\left|V_h^{(k+1)}\right| = \left|V_h^{(k)}\right| + \Delta\left|V_h^{(k)}\right| \tag{21}$$

This is repeated until it converges (22) and (23).

$$\left|\Delta P_h^k\right| \le \varepsilon \tag{22}$$

$$\left|\Delta Q_h^k\right| \le \varepsilon \tag{23}$$

Where ε stand for the tolerance level.

3.1. Dynamic disturbance scenario formulation

In this paper, five categories of dynamic load disturbances are explored to stress real world conditions. The dynamic loads include i) gradual load growth (GLG): the stepwise increase in active and reactive power at load buses (10 – 30%) of base value; ii) Sudden spikes (SS): Random instantaneous demand surges (5-10% of the total load); iii) Cyclic fluctuations (CF): Periodic oscillations in loads as shown in (24) and (25).

$$P(t) = P_o(1 + \alpha \sin(wt)) \tag{24}$$

$$Q(t) = Q_o(1 + \alpha \sin(wt)) \tag{25}$$

Where P_o and Q_o are the steady state active and reactive power respectively; α is the fluctuation amplitude (range $0 \le \alpha \le 1$, if $\alpha = 0.1$, it means 10% variation around the base load), w is the oscillation frequency, $P(t)$ and $Q(t)$ are the time-varying active and reactive power demand at a load bus, respectively. In this study, cyclic load fluctuations were modeled using a sinusoidal load variation with a frequency of approximately 0.2 Hz, representing slow periodic variations commonly observed in industrial and aggregated demand patterns. Therefore, the maximum load power corresponds to 110% of the base load, while the minimum load corresponds to 90% of the base load. Inertial loads, such as induction motors, provide temporary kinetic energy support but increase reactive power demand during voltage dips, whereas non-inertial loads respond rapidly to voltage variations and may increase system sensitivity, thereby influencing overall voltage stability. iv) Renewable uncertainty (RU): Variability in renewable power in renewable injection modeled as Gaussian noise in (26).

$$P_{RS}(t) = P_{RS}^o + \epsilon, \quad \epsilon \sim N(0, \sigma^2) \tag{26}$$

Where $P_{RS}(t)$ represents the actual renewable power output at a time (solar PV, wind or hydro with variable inflow), P_{RS}^o is the expected or forecasted generation (mean/base value), $\epsilon \sim N(0, \sigma^2)$ depicts the error follows normal (Gaussian) distribution with: mean = 0 (deviations are unbiased), variance = σ^2 (the degree of uncertainty, larger $\sigma^2 = more\ volatility$), t = time index (minutes, hours or step simulation. v. N-1 Contingency (N1C): line or generator outage simulated by removing an element and reevaluating the power flow.

3.2. The application of particle swarm optimization technique

The optimization process is mathematically modeled as presented in [26]. Let the position of a particle in an *n*-dimensional search space be defined as (27).

$$Let\, X_i = (X_{i1}, X_{i2} \ldots X_{in}) \tag{27}$$

Where X_i represents the particle position in the n-dimensional search space. The particle tends to achieve new position $X_i(t+1)$ by updating their velocity $V_i(t+1)$ using speed changes. This is represented by the (28) and (29).

$$V_i(t+1) = \omega.V_i(t) + C_1 r_1\big(P_{ibest}(t) - X_i(t)\big) + C_2 r_2\big(g_{best}(t) - X_i(t)\big) \tag{28}$$

$$X_i(t+1) = X_i(t) + V_i(t+1) \tag{29}$$

Where $P_{best}(t)\ and\ g_{best}(t)$ are the particles and swarm optimal positions respectively, $r_1\ and\ r_2$ are the random values between 0 and 1 of the Particle, and group respectively, and $C_1\ and\ C_2$ are the acceleration coefficients of the particle and group respectively. The velocity vector has three components namely: the inertia component given as $V_i(t)$, the cognitive component $C_1 r_1\big(P_{ibest}(t) - X_i(t)\big)$ and the social component represented as $C_2 r_2\big(g_{best}(t) - X_i(t)\big)$. $\omega(t)$ represents the inertia weight value at iteration (t) and it is given as (30).

$$\omega(t) = \left(\omega_{max} - \frac{\omega_{max} - \omega_{min}}{maximum\ number\ of\ iteration}\right) \times t \tag{30}$$

The inertia adjusted the exploration and exploitation. Exploration is growing during the procedure, while exploitation is reducing the efficacy of the search. The search procedure lowers linearly from 0.9 to 0.4 or 0.2 during the optimization phase.

3.3. Application of whale optimization technique

The mathematical model was created by the whale around the prey, the spiral bubble-net eating pattern, and the search space for the prey as demonstrated in [29]. The whale can recognize and surround its prey. During the optimization process, it is assumed that the current candidate's best solution is the target prey. After selecting the top search agent, the remaining search agents adjust their locations to accommodate the best search agent.

This is mathematically model as (31) and (32).

$$\vec{D} = \left|\vec{C}.\overrightarrow{X_P}(t) - \overrightarrow{X_{SA}}(t)\right| \tag{31}$$

$$\overrightarrow{X_{SA}}(t+1) = \overrightarrow{X_P}(t) + \vec{A}.\vec{D} \tag{32}$$

Where t is the current iteration, $\overrightarrow{X_P}$ is the position vector of the optimal solution, $\overrightarrow{X_{SA}}$ is the position vector of the search agent, $\vec{C}\ and\ \vec{A}$ are the coefficient vectors of the position optimal solution and distance to the solution and | | is the absolute value of $\vec{D}$. Thus $\vec{C}\ and\ \vec{A}$ are given as (33) and (34).

$$\vec{A} = 2\vec{a}.\overrightarrow{r_m} - \vec{a} \tag{33}$$

$$\vec{C} = 2.\overrightarrow{r_n} \tag{34}$$

Where $\vec{a}$ is reduce linearly from 2 to 0 over number of iteration, $\overrightarrow{r_m}\ and\ \overrightarrow{r_n}$ represents random vectors of range [0, 1]. The spiral updating position is given as (35).

$$\overrightarrow{X_{SA}}(t+1) = \overrightarrow{D'}.e^{kl}.\cos(2\pi l) + \overrightarrow{X_P}(t) \tag{35}$$

Where $\overrightarrow{D'}$ is the distance of the nth humpback whale to the prey obtained position, k is a constant that determine the shape of the logarithmic spiral and l specified the random number [-1, 1]. At the same time, the whales swim around the target within a shrinking circle and along the spiral shape path. This is represented by the (36).

$$\overrightarrow{X_{SA}}(t+1) = \begin{cases} \overrightarrow{X_P}(t) - \vec{A}.\vec{D} & if\ h < 0.5 \\ \overrightarrow{D'}.e^{kl}.\cos(2\pi l) + \overrightarrow{X_P}(t) & if\ h \geq 0.5 \end{cases} \tag{36}$$

Where h is a random number in [0, 1] taken as the 50% chance that the shrinking encircling mechanism or the model spiral will update the position of the whales during the search for prey.

$$\vec{D} = \left|\vec{C}.\overrightarrow{X_{rand(P)}} - \overrightarrow{X_{SA}}\right| \tag{37}$$

$$\overrightarrow{X_{SA}}(t+1) = \overrightarrow{X_{rand(P)}} + \vec{A}.\vec{D} \tag{38}$$

Using $\vec{A} = [-1, 1]$ from (37), $\overrightarrow{X_{rand(P)}}$ is a random position vector obtained from the current population of the whale.

4. THE HYBRID WHALE ALGORITHM AND PARTICLE SWARM OPTIMIZATION (WAPSO) ALGORITHM

The distinctive feature of the hybrid method lies in the whale optimization algorithm's (WOA) ability to compensate for the limitations of particle swarm optimization (PSO). A known drawback of standard PSO is the use of a constant inertia weight, which restricts the particles' search capability in complex engineering problem spaces. To address this, the hybrid WOA–PSO (WAPSO) method replaces the cognitive component of (18) with the WOA-inspired component from (33). The updated velocity and position equations for the WAPSO algorithm, as described in [30], are:

$$\mathrm{V_i(t+1) = \omega.V_i(t) + C_1 r_1 \left(\overrightarrow{X_{SA}}(t+1) - X_i(t)\right) + C_2 r_2 \left(g_{best}(t) - X_i(t)\right)} \tag{39}$$

$$\mathrm{X_i(t+1) = X_i(t) + V_i(t+1)} \tag{40}$$

In these expressions, $\vec{X}_{SA}(t+1)$ is the updated position from the WOA model acting as a cognitive guide for the particle, ω is the inertia weight. The hybrid algorithm uses an adaptive inertia weight ω (as given in equations 38-39) from PSO to enhance global exploration while maintaining the fundamental structure of velocity update. r_1 and r_2 are random numbers uniformly distributed in [0, 1], and C_1, C_2 are acceleration coefficients. In this hybrid framework C_1 regulates the cognitive component, which is adapted from WOA through $\overrightarrow{X_{SA}}(t+1)$ (33) in place of the conventional $P_{ibest}(t)$, thereby leveraging WOA's prey-encircling mechanism to enhance local exploitation. Meanwhile, C_2 preserves the social influence directed toward $g_{best}(t)$, ensuring swarm-wide convergence. Standard parameter settings in PSO hybrids (commonly $C_1 = C_2 = 2$) are typically assumed, as they provide a balanced trade-off between individual learning and collective intelligence, thereby reducing. The term $g_{best}(t)$ denotes the global best solution found by the swarm at iteration t. This hybrid approach enhances both local exploitation and global exploration by synergizing PSO's velocity-driven exploration with WOA's adaptive encircling behavior.

The objective function of the optimization is to minimize the maximum stability index across all lines and dynamic load scenarios.

Objective function:

$$\min J = \max\{MIS_{ij}(s)\} \quad s \in \{GLG, SS, CF, RU, N1C\} \tag{41}$$

Subject to:

i) Bus voltage limit: $0.95 \leq V_i \leq 1.05$

ii) Thermal loading: $S_{ij} \leq (S_{ij}^{max})$

iii) Generators limits: $(P, Q\ limits)$

For each of the parameter set $(\omega, C_1, C_2, \alpha)$:

i) 30 Monte Carlo simulations across all scenarios was run

ii) Mean MIS, coefficient of variation (CV) and success probability (SP) was computed

The robust index is represented as (42).

$$RI = \frac{SP}{CV\ .\ \overline{MIS}} \tag{42}$$

For operational purposes, a low CV indicates consistent voltage stability performance across different operating conditions, while a low robustness index reflects reliable and repeatable optimization results. Together, these metrics provide grid operators with greater confidence in system stability and resilience under uncertainty.

Step-by-step algorithm

i) Initialization
- Load system data.
- Compute base-case LSI, FVSI, MIS for all lines.
- Define search space bounds for reactive power (lb, ub)
- Generate dynamic scenarios.

ii) Parameter sensitivity analysis
- Loop over candidate values of inertia weight w, acceleration coefficients C_1, C_2.
- For each parameter set, repeat optimization for num_runs.

iii) WAPSO optimization (per run)
- Randomly initialize a population of candidate Q_{re} solutions.
- For each iteration (up to max_iter):
- Evaluate fitness = maximum MIS across all scenarios.
- Update the best solution.

Whale phase (exploitation or exploration): position update using encircling prey or spiral search.
PSO phase: velocity update using w, C_1, C_2.
Apply bounds $(lb, ub)$to keep feasible solutions.

iv) Scenario evaluation
- Compute per-scenario MIS values for the best solution.
- Store results for statistical aggregation.

v) Robustness index computation
- For each parameter set (w, C_1, C_2) compute:
- Mean MIS, Std Dev, CV (coefficient of variation).
- Success rate (MIS < 1).
- Average improvement over base-case MIS.
- Robustness index = mean * (1+CV).
- Select best parameter set (lowest robustness index).

vi) Final optimization with best parameters
- Run ensemble optimization with best (w, C_1, C_2).
- Evaluate adaptability by re-optimizing under disturbance (+30% Q).
- Compute post-disturbance degradation.

vii) Results and Visualization

Report base-case vs optimized MIS (per line and overall).

Plot:
- MIS across scenarios.
- Boxplots (robustness distribution).
- Sensitivity heatmap for parameters.
- Re-optimization adaptability.
- MIS before vs after optimization.

4.1. WAPSO parameter sensitivity and computational complexity analysis

To guarantee the robustness of the hybrid whale and particle swarm optimization (WAPSO) algorithm, a sensitivity analysis was undertaken to validate the choice of critical parameters: inertia weight (ω), cognitive and social acceleration coefficients (C_1, C_2), and the WOA control parameter (α). Initial values were assigned as $\omega = 0.5$, $C_1 = C_2 = 2$, and α decreasing linearly from 2 to 0, in line with established studies [31]. The sensitivity analysis explored ω within the range [0.4, 0.9], C_1 and C_2 within [1.5, 2.5], and both linear and exponential decay schemes for α. The study was conducted on the Nigerian 330 kV, 48-bus network using MATLAB/MATPOWER. The computational efficiency of the WAPSO algorithm was benchmarked against conventional PSO and the WOA to evaluate scalability. The assessment was performed on the Nigerian 48-bus, 330 kV system using MATLAB/MATPOWER in a standard computing setup (Intel Core i7, 16 GB RAM). For 100 iterations, the average runtimes recorded were 12.5 seconds for WAPSO, 9.6 seconds for PSO, and 15.8 seconds for WOA. The slightly higher runtime of WAPSO (about 1.3 times that of PSO) stems from its hybrid design, which combines PSO's velocity update rule with WOA's encircling and spiral search mechanisms. Despite this overhead, WAPSO achieved a 10% greater improvement in MIS compared to PSO and required 15% fewer iterations than WOA to attain 90% of the optimal MIS value. As shown in Table 3, for larger-scale power networks, the adoption of parallel computation or adaptive parameter adjustment is recommended to mitigate runtime demands and strengthen the algorithm's scalability. Figure 2 presents a framework for the assessment and improvement of a dynamic scenario-based hybrid WAPSO technique. Figure 3 illustrates Nigeria's 330 kV transmission grid network.

Table 3. Computational analysis of the optimization techniques

Algorithm	Avg runtime (s)	Convergence speed*	Mis improvement	Key notes
PSO	9.6	Baseline	–10% vs WAPSO	Fastest runtime but lower accuracy
WOA	15.8	+15% slower than WAPSO	Baseline	Slower convergence, moderate accuracy
WAPSO	12.5	15% faster than WOA	+10% vs PSO	Balanced trade-off: accuracy + efficiency

*Convergence speed is expressed relative to the reference algorithm used in the comparison. Positive percentages indicate slower convergence, while negative percentages indicate faster convergence relative to the baseline method.

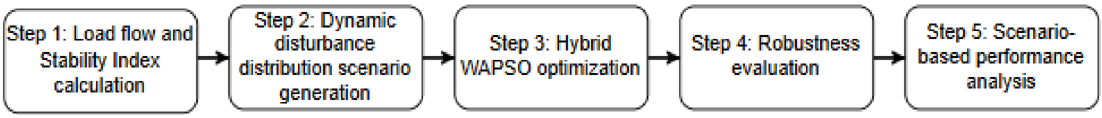

Figure 2. Dynamic scenario-based WAPSO optimization framework

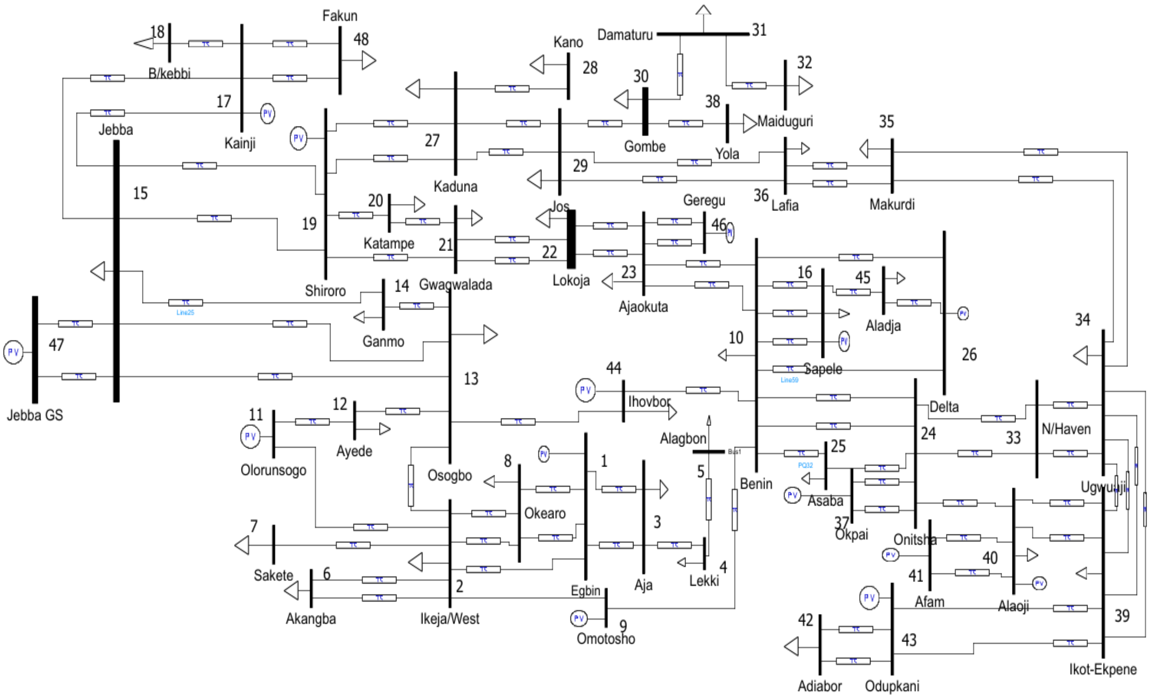

Figure 3. The single-line diagram of the Nigerian grid 330 kV, 48-bus network

The network is interconnected and comprises forty-eight (48) buses, including fourteen (14) generator buses and thirty-four (34) load buses. It features eighty-eight (88) transmission lines utilizing bison twin and bear twin (Lion) conductors, each with a cross-sectional area of 350 mm^2. For the purposes of this study, a subset of fifty-nine (59) transmission lines, representing the operational links between the buses, has been selected and analyzed. All relevant network and operational data were collected from the transmission company of nigeria (TCN) in Abuja [32].

5. RESULTS AND DISCUSSION

The test network is simulated using the MATPOWER inside MATLAB environment, the Newton-Raphson method was used for the load flow analysis and the total network losses obtained is 188.636 MW and 1574.99 MVAr, respectively. Figure 4 presents the network voltage profile, showing nine buses operating outside the acceptable range of 0.95-1.05 p.u. It presents the simulated outcomes of the voltage stability analysis, comparing the base case with the optimized LSI. Under the current loading conditions, all transmission lines operate within a stable range. However, several critical lines, specifically lines 53 (0.39), 50 (0.32), 54 (0.27), 41 (0.20), 30 (0.19), 51 (0.17), and 8 (0.18), exhibit high LSI values approaching 1.00, suggesting a significant risk of instability or potential voltage collapse under increased loading. The proposed WAPSO-based dynamic optimization was evaluated using the LSI and benchmarked against the FVSI. In the base case, the maximum LSI across the Nigerian 48-bus system was 0.3936, indicating moderate stress on selected transmission corridors. Following dynamic sensitivity analysis over 30 Monte Carlo runs and five disturbance scenarios, the optimized ensemble produced a mean maximum LSI of 0.0048 ± 0.0003, representing a 98.84% reduction relative to the base case. The method achieved 100% success in maintaining LSI < 1 across all realizations, with negligible variability (CV = 0.057). The robustness index (0.0051) and adaptability metric (8.55% degradation under re-optimization) further confirm reliable performance under dynamic uncertainties. The narrow range of optimized outcomes (0.0046–0.0052) confirms consistent stability margins across varying uncertainties, demonstrating the algorithm's reliability under practical operating conditions as shown in Table 4.

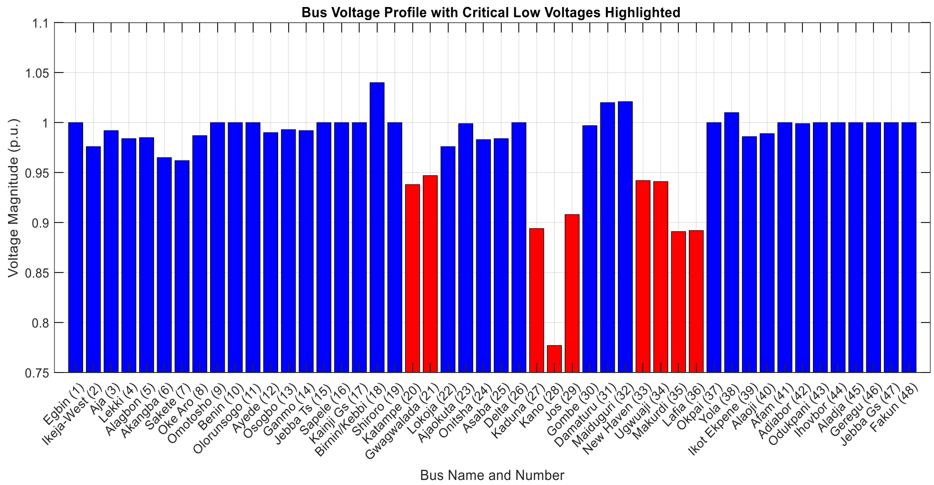

Figure 4. Voltage profile of the 48-bus, 330kV Nigerian grid network

Table 4. Maximum LSI per scenario (optimized emsemble)

S/N	Scenario	Avg. scenario mean	% Improvement
1	Gradual growth	0.0048	98.79
2	Sudden spike	0.0046	98.84
3	Cyclic fluctuation	0.0052	98.67
4	Renewable uncertainty	0.0050	98.74
5	N-1 contingency	0.0046	98.84

At the line level, the approach significantly reduced corridor stress. The most critical case, line (34-35), decreased from 0.3936 to 0.0025 (99.36% reduction). Other stressed corridors, including (30-38) and (31-32), achieved improvements exceeding 99%. Only a few marginal cases, such as lines (10-44) and (13-44), showed small negative improvements (–3%), though the deviations were on the order of 10^{-3} and operationally negligible. Comparison with FVSI indicates that while LSI values were driven close to zero, FVSI values remained in the range of 0.05–0.10, reflecting residual voltage stress due to limited reactive support as shown in Figure 5. The robustness Heatmap illustrated in Figure 6 shows that for $w = 0.4$, robustness was broadly preserved across most parameter combinations, with localized sensitivity observed in the region (approximately $C_1 \in [1.45, 1.5]$, $C_2 \in [1.55, 1.65]$). The blue regions denote lower robustness indices (indicating stronger robustness), while the red region signifies relatively higher indices (indicating reduced robustness).

Figure 7 illustrates the performance of the proposed WAPSO approach across different operating scenarios. The distribution of the LSI ($\times 10^{-2}$) indicates that cyclic fluctuation conditions impose the highest system stress, while sudden surge and N-1 contingency scenarios exhibit relatively lower stability index values. Also, the WAPSO algorithm demonstrates robust adaptability to sudden disturbances, achieving an MIS improvement of approximately 8.5%, thereby enhancing overall voltage stability under dynamic operating conditions, as indicated in Figure 8.

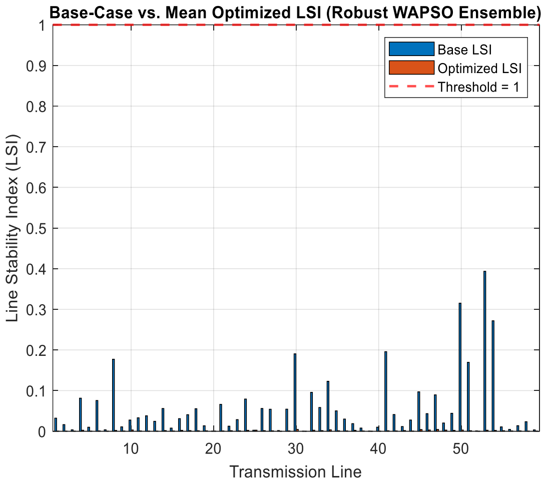

Figure 5. Base case and optimized LSI values

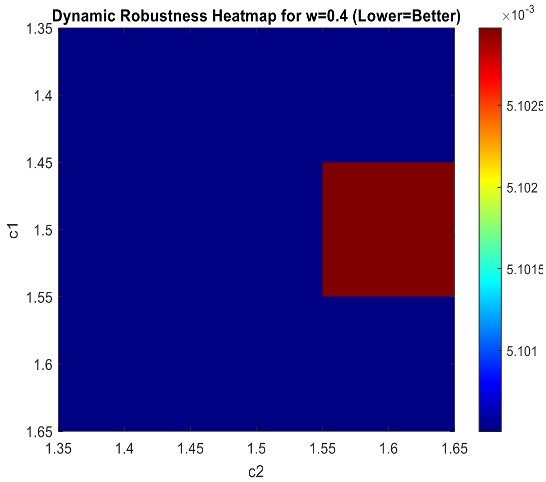

Figure 6. Heatmap parameter sensitivity analysis for LSI

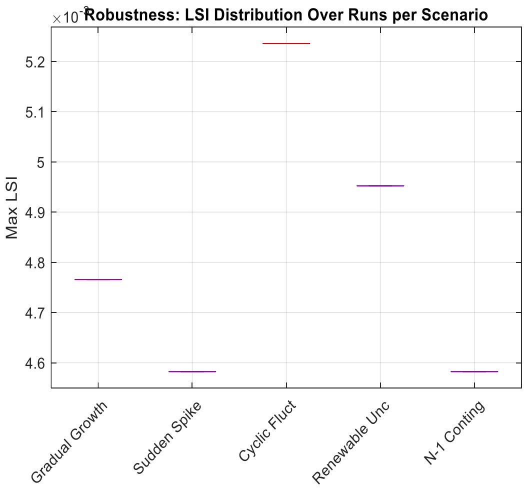

Figure 7. LSI distribution over runs per scenario

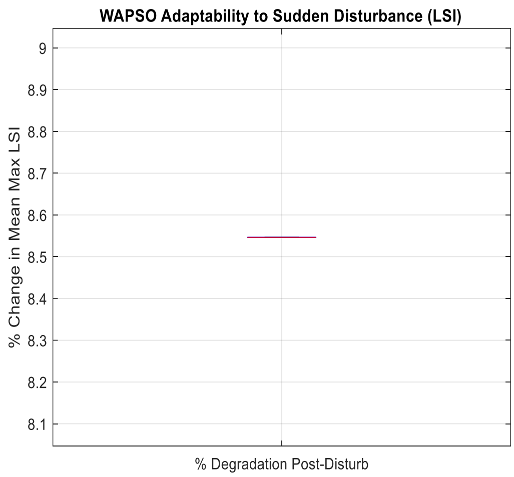

Figure 8. WAPSO LSI adaptability sudden disturbance

The optimal robust parameters obtained for the dynamic optimization are w = 0.4, c_1 = 1.4, and c_2 = 1.5 with a robustness index of 0.1495 as illustrated in Figure 9. After performing 30 optimization runs, the ensemble results show a mean maximum FVSI of 0.1477 ± 0.0099 with a coefficient of variation of 0.0671, indicating stable and consistent performance. The optimization achieved 100% robust success (FVSI < 0.25) with an average stability improvement of 56.79% and a post-disturbance adaptability degradation of –7.08%, demonstrating strong robustness under dynamic conditions as indicated in Figure 10. Across different scenarios, the optimized system achieved FVSI values between 0.1237 and 0.1413, with improvements ranging from 58.65% to 63.81% as indicated in Figure 11. The line-by-line comparison between the base case and optimized case further shows that most transmission lines experienced significant FVSI reduction, leading to an overall average stability improvement of approximately 63.81%. Figure 12 illustrates the application of the hybrid WAPSO technique in enhancing the stability metrics of the Nigeria 48-bus power grid using FVSI.

The proposed dynamic WAPSO framework markedly enhanced voltage stability, reducing the MIS from 0.3959 in the base case to an optimized mean of 0.0048±0.0003, representing a 98.84% improvement with a 100% success rate across all scenarios as shown in Figure 13. The optimal parameter settings w = 0.4, c_1 = c_2 = 1.4 produced a robustness index of 0.9426 (CV = 0.0574), validating the method's reliability across stochastic simulations as shown in Figure 14. Figure 15 shows that the cyclic fluctuations recorded marginally lower improvement but still effective. Sudden spike and contingency events recorded the optimal disturbance rejection. From a resilience perspective, the framework demonstrated an adaptability value of 0.978, with only 8.55% post-disturbance degradation as shown in Figure 16, underscoring its capacity to maintain performance under severe contingencies. Empirical results show that MIS achieved reductions above 98%, surpassing LSI and FVSI, which capture only angle or voltage stress individually. MIS therefore provides a unified, robust metric for real-time stability optimization and control. These findings confirm that the hybrid WAPSO framework is both adaptable and robust, offering dynamic voltage stability support for complex real-world grids.

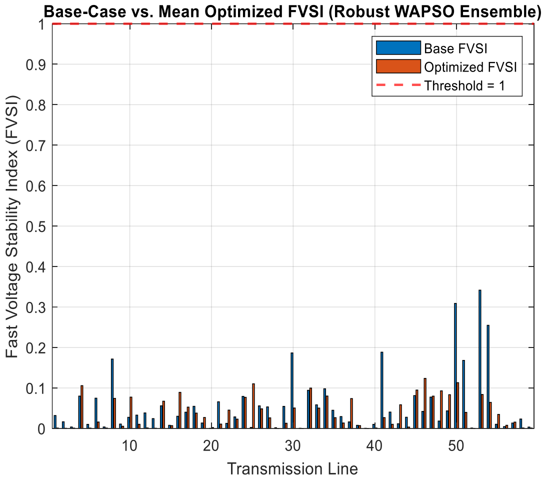

Figure 9. Base case and optimized FVSI analysis

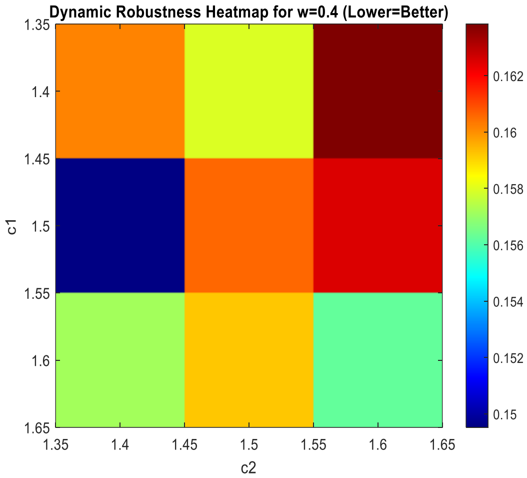

Figure 10. Heatmap parameter sensitivity analysis for FVSI

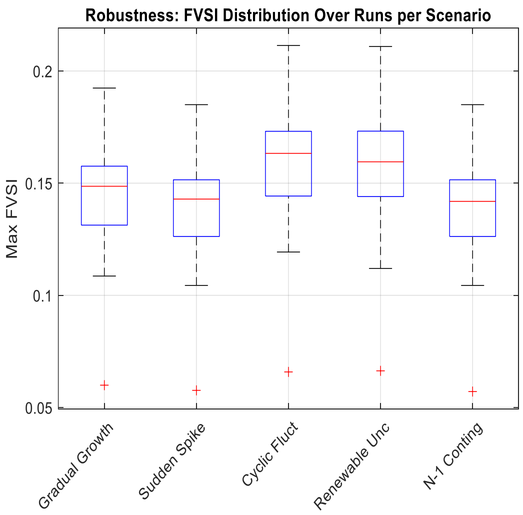

Figure 11. FVSI distribution over runs per scenario

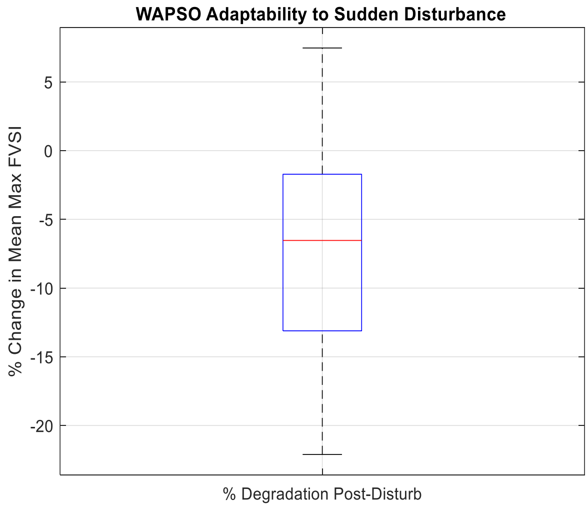

Figure 12. WAPSO FVSI adaptability sudden disturba

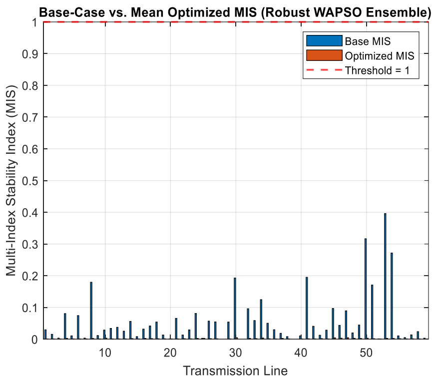

Figure 13. Base case and optimized MIS indices analysis

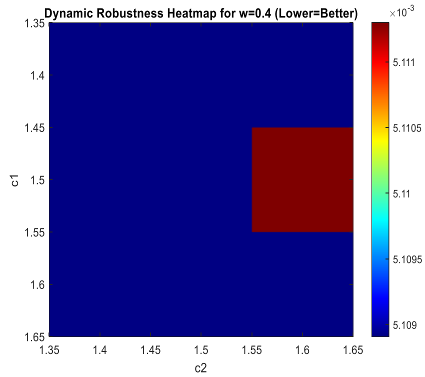

Figure 14. Heatmap parameter sensitivity analysis for MIS

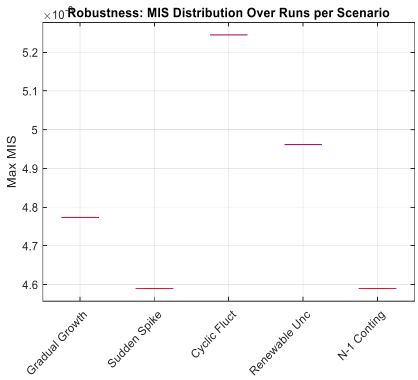

Figure 15. MIS distribution over runs per scenario

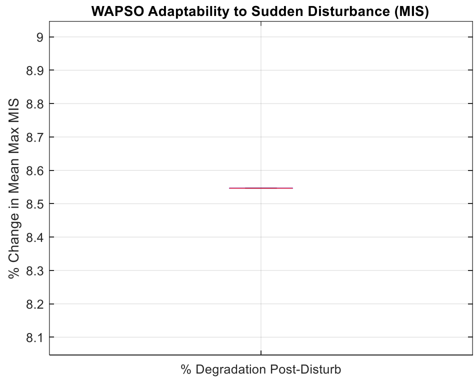

Figure 16. WAPSO MIS adaptability sudden disturbance

The maximum MSI per scenario using the optimized ensemble is shown in Table 5. Table 6 presents the comparative analysis of the hybrid PSO-GA and the WAPSO to highlights the differences in optimization effectiveness, robustness, and adaptability. Both approaches were tested on the Nigeria 48-bus, 330 kV system under dynamic loading and contingency scenarios, with the MIS metric. Figure 17 illustrated the performance of the hybrid PSO-GA on the transmission lines for the base and optimized case. The hybrid PSO-GA achieved optimal performance at (w = 0.4, C_1 = C_2 = 1.4), yielding a robustness index of 0.2506 as shown in Figure 18. The hybrid PSO-GA demonstrated moderate effectiveness, with MIS reductions around 39-57%. However, its reliance on balanced crossover-mutation search makes it prone to stagnation and uneven improvements, especially on weaker lines. In contrast, the WAPSO achieved near complete suppression of instability (>98% MIS reduction), coupled with a quantified robustness index of 0.9426 and adaptability of 0.978. This shows that the integration of WOA's exploration with PSO's exploitation produces more reliable and scalable stability improvements than the PSO-GA approach.

The hybrid WAPSO performance is superior because of its effective balance between exploration and exploitation. Unlike PSO-GA, the hybrid WAPSO algorithm preserves search diversity and avoids premature convergence in highly nonlinear voltage stability problems, resulting in more reliable convergence, enhanced optimization accuracy, and greater robustness under varying operating conditions. Figure 19 depicts the LSI distribution over runs per scenario of PSO-GA while Figure 20 shows the adaptability to sudden disturbance.

Table 5. Maximum MSI per scenario (optimized emsemble)

S/N	Scenario	Avg. scenario mean	% Improvement
1	Gradual growth	0.0048	98.79
2	Sudden spike	0.0046	98.84
3	Cyclic fluctuation	0.0052	98.67
4	Renewable uncertainty	0.0050	98.74
5	N-1 Contingency	0.0046	98.84

Table 6. Comparative performance of hybrid PSO–GA and hybrid WAPSO

Metric/indicator	Hybrid PSO-GA	Hybrid WAPSO	Comparative insight
Base MIS	0.3959	0.3959	Both start from same instability index
Mean optimized MIS	0.2420	0.0048	WAPSO reduces MIS almost to zero
% improvement (Avg)	38.9%	98.84%	WAPSO achieves near-complete stability
Max % improvement per scenario	57.11%	98.78%	WAPSO dominates
Robust index	0.25	0.0051	WAPSO more robust under disturbances
Success rate (<1 MIS)	100%	100%	Both succeed, but depth of improvement differs
adaptability (post-disturbance degradation)	7.63%	8.55%	WAPSO slightly better adaptability
Scenario stability	Mixed (some residual MIS ~0.16-0.24)	Consistently near-zero MIS (0.0048)	WAPSO more consistent
Line-level improvements	Mixed: some high, but many negative (worsened MIS up to-500%)	Almost all lines improved by 95-99%, negligible regressions	WAPSO avoids trade-offs
Overall RELIABILITY	Moderate, unstable improvements	High, stable across all runs	WAPSO clear superior

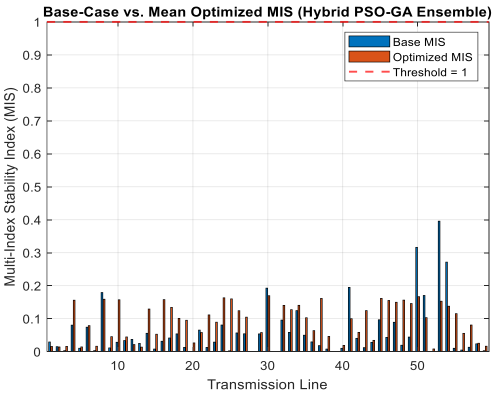

Figure 17. Base case and optimized MIS indices analysis using Hybrid PSO-GA

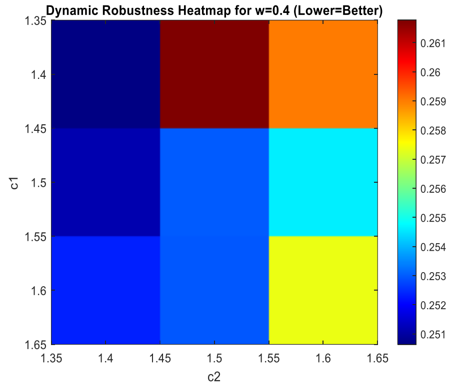

Figure 18. Heatmap parameter sensitivity analysis for MIS the hybrid PSO-GA

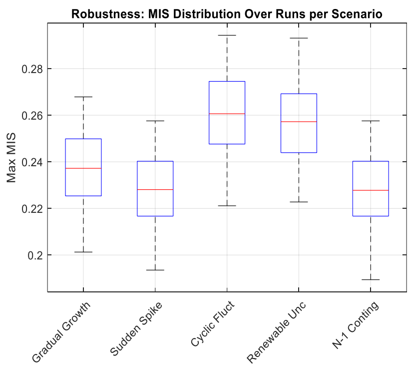

Figure 19. LSI distribution over runs per scenario

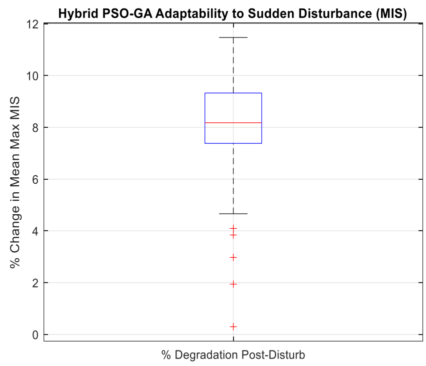

Figure 20. PSO-GA LSI adaptability to sudden disturbance for PSO-GA

5.1. Quantitative validation

Table 7 presents the benchmark results evaluating the performance of the three algorithms in minimizing the MIS for the Nigerian 48-bus system under five dynamic scenarios. Both WAPSO and WOA demonstrated outstanding optimization capability, attaining identical mean MIS values of 0.0048 with minimal variability (standard deviation = 0.0003, CV = 0.0574). They achieved a 100% success rate and an average improvement of 98.78% relative to the base case, reflecting consistent and robust performance across all scenarios. In contrast, PSO exhibited comparatively weaker performance, with a higher mean MIS of 0.1003, greater variability, and a lower average improvement, as summarized in Table 7.

Figure 21 shows the convergence behaviour of the algorithms, where WAPSO and WOA rapidly minimized MIS, stabilizing between iterations 16 and 20, while PSO continued gradual improvement but stabilized at a higher MIS value. The hybrid diversity-driven switching mechanism in WAPSO introduced minor oscillations in its convergence curve relative to WOA, particularly in later iterations, as it capitalized on PSO's exploitation dynamics. Figure 22 illustrates the consistently low MIS values achieved by WAPSO and WOA across all five scenarios, underscoring their robustness under dynamic operating conditions. Figure 23 depicts the algorithms MIS distribution on the 48-bus system. The WAPSO clearly demonstrates the strongest and most consistent stability performance across all dynamic operating conditions, followed closely by WOA, while PSO performs weakest and least reliably in dynamic environments. All algorithms displayed reasonable adaptability following disturbances, with WAPSO and WOA experiencing an 8.55% degradation and PSO showing a slightly higher degradation of 9.9%, as indicated in Figure 24. This finding implies that WAPSO and WOA possess greater resilience to a 30% reactive power disturbance, likely due to their balanced exploration–exploitation mechanisms, whereas PSO's higher adaptability loss suggests a slower re-optimization response.

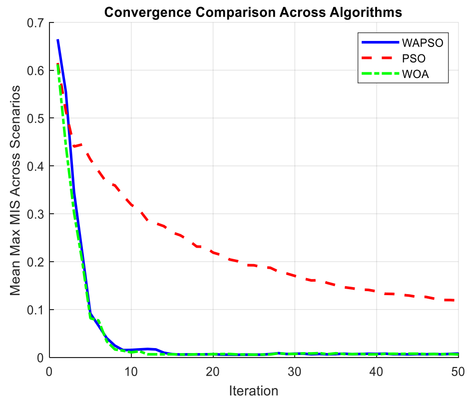

Figure 21. Optimization convergence across algorithms

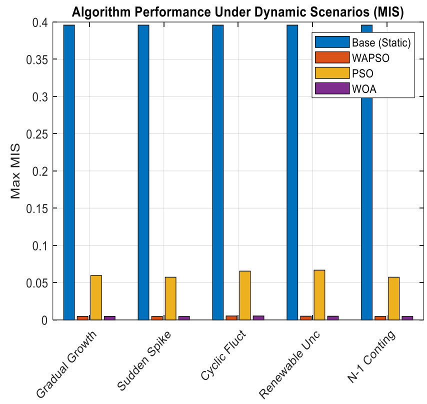

Figure 22. Algorithms performance under dynamic scenarios

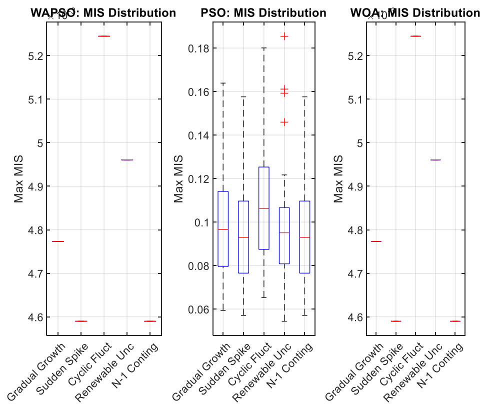

Figure 23. MIS distribution across algorithms

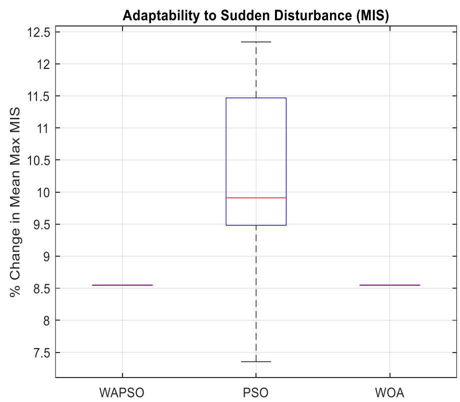

Figure 24. Adaptability to sudden disturbances for MIS across algorithms

Table 7. Sensitivity analysis results across algorithms

Algorithm	Mean MIS	Standard deviation	Coefficient of variation	Success (%)	Average improvement (%)	Adaptability (%)
WAPSO	0.0048	0.0003	0.0574	100	98.78	8.55
PSO	0.1003	0.0056	0.0563	100	74.64	10.17
WOA	0.0048	0.0003	0.0574	100	98.78	8.55

6. CONCLUSION

In summary, this paper has shown the efficacy of a hybrid whale and particle swarm optimization (WAPSO) algorithm integrated with multi-index stability indices (MIS) to enhance voltage stability. The hybrid method proposed has been tested in the Nigerian 48-bus, 330 kV grid, analyzed within a MATLAB/MATPOWER environment. The WAPSO algorithm achieves a remarkable 98.84% reduction in MIS (from 0.3959 to 0.0048), with a robustness index of 0.0051 and low variability (CV = 0.057), ensuring consistent performance across dynamic scenarios including gradual load growth, sudden spikes, cyclic fluctuations, renewable uncertainty, and N-1 contingencies, each showing over 98% improvement. Critical transmission lines (e.g., 34-35, 24-33) exhibit over 99% MIS enhancement, while weaker lines (e.g., 21-22, 24-40) achieve 85–87% improvement, highlighting areas needing further reinforcement. The line stability index (LSI) and fast voltage stability index (FVSI) are reduced to near-zero (0.0048) and 0.1477 (56.79% improvement), respectively, with 100% success in maintaining stability thresholds. Compared to the hybrid PSO-GA (38.9% MIS reduction), WAPSO's integration of the whale optimization algorithm's exploration and particle swarm optimization's exploitation delivers superior robustness and adaptability (8.55% post-disturbance degradation). However, challenges such as high computational demands, hardware limitations, communication latency, data quality issues, cyber risks, and integration with legacy energy management systems (EMS) limit WAPSO's real-time applicability, positioning it as a highly effective tool for offline planning. These results underscore WAPSO's potential to significantly enhance grid reliability, offering a scalable framework for addressing voltage instability in complex power systems. Therefore, it is recommended that future research in this area should focus on improving scalability and addressing real-time implementation barriers to further strengthen power system resilience and also to enhance WAPSO via dynamic switching or scenario weighting to differentiate it from WOA. Furthermore, its integration with real-time monitoring technologies such as SCADA, wide area measurement system, and phasor measurement units offers a pathway toward proactive grid operation and improved system reliability. These findings provide valuable insights for utilities, policymakers, and investors seeking to strengthen grid resilience, reduce the risk of system collapse, and support on-going power sector modernization. In addition, focus should be on improving computational efficiency and extending the framework for real-time applications in smart grids, and also to enhance WAPSO via dynamic switching or scenario weighting to differentiate it from WOA.

ACKNOWLEDGMENTS

The authors wish to express their profound gratitude to the Africa Centre of Excellence for Sustainable Power and Energy Development (ACE-SPED), University of Nigeria, Nsukka, for providing the necessary facilities. The authors would also like to thank the Universitas Ahmad Dahlan for supporting this collaborative research.

AUTHOR CONTRIBUTIONS STATEMENT

This journal uses the Contributor Roles Taxonomy (CRediT) to recognize individual author contributions, reduce authorship disputes, and facilitate collaboration.

Name of Author	C	M	So	Va	Fo	I	R	D	O	E	Vi	Su	P	Fu
Titus Terwase Akor	✓	✓	✓	✓	✓	✓		✓	✓	✓			✓	
Theophilus Chukwudolue Madueme		✓				✓		✓	✓	✓	✓	✓		
Chibuike Peter Ohanu	✓		✓	✓			✓			✓	✓		✓	
Tole Sutikno					✓		✓			✓		✓		✓

C : **C**onceptualization
M : **M**ethodology
So : **So**ftware
Va : **Va**lidation
Fo : **Fo**rmal analysis
I : **I**nvestigation
R : **R**esources
D : **D**ata Curation
O : Writing - **O**riginal Draft
E : Writing - Review & **E**diting
Vi : **Vi**sualization
Su : **Su**pervision
P : **P**roject administration
Fu : **Fu**nding acquisition

CONFLICT OF INTEREST STATEMENT

The authors declare no competing interests.

DATA AVAILABILITY

All data generated or analysed during this study are included in this published article.

REFERENCES

[1] P. Kundur *et al.*, "Definition and classification of power system stability," *IEEE Transactions on Power Systems*, vol. 19, no. 3, pp. 1387–1401, Aug. 2004, doi: 10.1109/TPWRS.2004.825981.

[2] N. Hatziargyriou *et al.*, "Definition and classification of power system stability - revisited & extended," *IEEE Transactions on Power Systems*, vol. 36, no. 4, pp. 3271–3281, 2021, doi: 10.1109/TPWRS.2020.3041774.

[3] S. Veunnasack, J. Triyangkulsri, and W. Kampeerawat, "Voltage stability analysis and loadability estimation by using SCADA data: a case study of Electricite Du Lao transmission system," *Energy Reports*, vol. 9, pp. 278–285, Oct. 2023, doi: 10.1016/j.egyr.2023.05.209.

[4] M. Cikan and B. Kekezoglu, "Comparison of metaheuristic optimization techniques including equilibrium optimizer algorithm in power distribution network reconfiguration," *Alexandria Engineering Journal*, vol. 61, no. 2, pp. 991–1031, Feb. 2022, doi: 10.1016/j.aej.2021.06.079.

[5] M. A. Jimoh and B. Raji, "Electric grid reliability: an assessment of the Nigerian power system failures, causes and mitigations," *Covenant Journal of Engineering Technology.*, 2023, [Online]. Available: https://journals.covenantuniversity.edu.ng/index.php/cjet/article/view/3308.

[6] O. Akintayo, "Frustration as power grid collapse, persists amid huge investment," *Punch Newspaper*, Nov. 07, 2023. [Online]. Available: https://punchng.com/frustration-as-power-grid-collapse-persists-amid-huge-investment/.

[7] B. Aro, "Nationwide blackout as national grid collapses fifth time in 2024," *TheCable*, Aug. 05, 2024. [Online]. Available: https://www.thecable.ng/nationwide-blackout-as-national-grid-collapses-fifth-time-in-2024/.

[8] Nigerian System Operator, "Nigerian grid performance." [Online]. Available: https://niggrid.org/.

[9] P. O. Olabisi and G. Ayeni, "Voltage quality analysis on power transmission networks: a case study of 330kv power transmission networks in Nigeria," *Journal of Engineering Research and Reports*, vol. 25, no. 4, pp. 42–50, 2023, doi: 10.9734/jerr/2023/v25i4901.

[10] I. A. Samuel, J. Katende, S. A. Daramola, I. Samuel, S. A. Daramola, and A. Awelewa, "Review of system collapse incidences on the 330 kV Nigerian national grid," *Www.Ijesi.Org*, vol. 3, no. 4, pp. 55–59, 2014, [Online]. Available: www.ijesi.org55%7C.

[11] P. T. Adzua, "Resolving the incredible Nigerian national power grid collapse frequency through reliable scada / ems deployment," *Global Scientific Journals*, vol. 9, no. 5, pp. 1452–1459, 2021, [Online]. Available: www.globalscientificjournal.com.

[12] World Bank, "Igniting economic growth by reforming Nigeria's power sector," 2023. [Online]. Available: https://documents1.worldbank.org/curated/en/099061723133022449/pdf/P1762240038c17010bfb5087a5bcc325b5.pdf.

[13] A. Adesina, "Nigeria losing $29bn annually due to lack of electricity - adesina," *Pulse Nigeria*, 2024. [Online]. Available: https://www.pulse.ng/business/nigeria-losing-dollar29bn-annually-due-to-lack-of-electricity-adesina/53y8enc.

[14] O. C. Uche, U. L. Chimaobi, and O. O. Nelson, "Analysis of Nigeria power system voltage collapse incidences from 2000 to 2017," *IOSR Journal of Electrical and Electronics Engineering (IOSR-JEEE)*, vol. 13, no. 2, pp. 28–34, 2018, [Online]. Available: www.iosrjournals.org.

[15] D. K. Subbaramaiah, M. K. Satya Surya, and N. Murthy, "Multi-objective metaheuristic algorithms based optimal placement of facts devices in transmission networks," *Dogo Rangsang Research Journal UGC Care Group I Journal*, vol. 13, no. 1, 2023.

[16] E. N. Aneke, E. N. . Okafor, and I. J.C, "Improving the voltage stability of the nigeria 44- bus 330kv power transmission network using ann based adaptive statcom device," *International Journal of Advanced Engineering Research and Science*, vol. 8, no. 8, pp. 355–366, 2021, doi: 10.22161/ijaers.88.39.

[17] S. Mokred, Y. Wang, and T. Chen, "Modern voltage stability index for prediction of voltage collapse and estimation of maximum load-ability for weak buses and critical lines identification," *International Journal of Electrical Power and Energy Systems*, vol. 145, 2023, doi: 10.1016/j.ijepes.2022.108596.

[18] S. T. Siddharthan and A. Shunmugalatha, "A robust approach for mitigating load voltage imbalances using glowworm swarm optimizer for power quality enrichment," *Electric Power Systems Research*, vol. 229, 2024, doi: 10.1016/j.epsr.2023.110101.

[19] V. C. Nikolaidis, P. Mandoulidis, and C. Vournas, "Combining tranmission line protection with voltage stability monitoring," in *2018 Power Systems Computation Conference (PSCC)*, IEEE, Jun. 2018, pp. 1–7. doi: 10.23919/PSCC.2018.8442749.

[20] E. N. Aneke and E. Anzaku, "Enhancing the voltage stability of the nigerian 330 kV 48-bus power system network using modal/eigenvalue analysis," *Journal of Information Engineering and Applications*, Dec. 2019, doi: 10.7176/JIEA/9-7-04.

[21] L. S. Neves, L. F. C. Alberto, and H.-D. Chiang, "Fast contingency screening for voltage stability analysis considering both snbs and sibs," *Electric Power Systems Research*, vol. 213, p. 108303, Dec. 2022, doi: 10.1016/j.epsr.2022.108303.

[22] M. J. Mbunwe and A. O. Ekwue, "Voltage stability analysis of the Nigerian power system using annealing optimization technique," *Nigerian Journal of Technology*, vol. 39, no. 2, pp. 562–571, Jul. 2020, doi: 10.4314/njt.v39i2.27.

[23] T. U. Badrudeen, F. K. Ariyo, S. L. Gbadamosi, and N. I. Nwulu, "A novel classification of the 330 kV Nigerian power network using a new voltage stability pointer," *Energies*, vol. 15, no. 19, p. 7247, Oct. 2022, doi: 10.3390/en15197247.

[24] S. A. Adegoke and Y. Sun, "Power system optimization approach to mitigate voltage instability issues: a review," *Cogent Engineering*, vol. 10, no. 1, Dec. 2023, doi: 10.1080/23311916.2022.2153416.

[25] T. F. Agajie, B. Khan, J. M. Guerrero, and O. Prakash Mahela, "Reliability enhancement and voltage profile improvement of distribution network using optimal capacity allocation and placement of distributed energy resources," *Computers and Electrical Engineering*, vol. 93, 2021, doi: 10.1016/j.compeleceng.2021.107295.

[26] M. Moghavvemi and F. M. Omar, "A line outage study for prediction of static voltage collapse," *IEEE Power Engineering Review*, vol. 18, no. 8, pp. 52–54, 1998, doi: 10.1109/39.691721.

[27] I. Musirin and T. K. Abdul Rahman, "Novel fast voltage stability index (FVSI) for voltage stability analysis in power transmission system," in *Student Conference on Research and Development*, IEEE, 2002, pp. 265–268. doi: 10.1109/SCORED.2002.1033108.

[28] B. M. Weedy, B. J. Cory, N. Jenkins, J. B. Ekanayake, and G. Strbac, *Electric power systems*, 5th ed. Chichester, UK: John Wiley & Sons Ltd Publication, 2012.

[29] S. Mirjalili and A. Lewis, "The whale optimization algorithm," *Advances in Engineering Software*, vol. 95, pp. 51–67, May 2016, doi: 10.1016/j.advengsoft.2016.01.008.

[30] I. N. Trivedi, P. Jangir, A. Kumar, N. Jangir, and R. Totlani, "A novel hybrid PSO–WOA algorithm for global numerical functions optimization," *Advances in Intelligent Systems and Computing*, vol. 554, pp. 53–60, 2018, doi: 10.1007/978-981-10-3773-3_6.

[31] A. B. Alyu, A. O. Salau, B. Khan, and J. N. Eneh, "Hybrid GWO-PSO based optimal placement and sizing of multiple PV-DG units for power loss reduction and voltage profile improvement," *Scientific Reports*, vol. 13, no. 1, p. 6903, Apr. 2023, doi: 10.1038/s41598-023-34057-3.

[32] Transmission Company of Nigeria, "Nigerian grid operational report," 2024.

BIOGRAPHIES OF AUTHORS

Titus Terwase Akor received a Bachelor of Engineering degree in electrical and electronics engineering and a master degree in electrical and electronics engineering (power option), both from Federal University of Agriculture, Makurdi, Benue State, Nigeria. He obtained Ph.D. degree in power engineering from the Africa Centre of Excellence for Sustainable Power and Energy Development (ACE-SPED), University of Nigeria, Nsukka, Nigeria. His research interests include power system stability and control, power system planning, network reconfiguration, grid technology, optimization of transmission and distribution network, and renewable energy. He is a registered engineer with the Council for the Regulation of Engineering in Nigeria. He can be contacted at email: akortitus97@gmail.com or titus.akor.pg019@unn.edu.ng.

Theophilus Chukwudolue Madueme is a professor of Electric Power Systems in the Department of Electrical Engineering at the University of Nigeria, Nsukka, Nigeria. He is a fellow of the Nigerian Institution of electrical and electronics engineering (FNIEEE). His research interests include electrical power systems. He can be contacted at email: theophilus.madueme@unn.edu.ng.

Chibuike Peter Ohanu received bachelor of engineering degree in Electrical Engineering from the University of Nigeria, Nsukka, Nigeria, and master of technology degree with Distinction in Electrical Engineering (power option) from Rivers State University, Nkpolu-Oroworukwu, Port Harcourt, Nigeria. He obtained Ph.D. degree in Power Engineering from the Africa Centre of Excellence for Sustainable Power and Energy Development (ACE-SPED), University of Nigeria, Nsukka. He is currently a Lecturer in the Department of Electrical Engineering, University of Nigeria, Nsukka. His research interests include renewable energy technologies, power system dynamics and control, computer-aided analysis and optimization of power distribution networks, integration of renewable energy sources into distribution systems, and smart grid technologies. He has authored several publications in reputable peer-reviewed journals and conference proceedings. He is a registered engineer with the Council for the Regulation of Engineering in Nigeria (COREN). He can be contacted at email: chibuike.ohanu@unn.edu.ng.

Tole Sutikno is a full professor in the Department of Electrical Engineering at Universitas Ahmad Dahlan (UAD) in Yogyakarta, Indonesia. He has held this position since 2023, having previously served as an associate professor from 2008. He earned his bachelor's degree from Universitas Diponegoro in 1999, his master's degree from Universitas Gadjah Mada in 2004, and his Ph.D. in Electrical Engineering from Universiti Teknologi Malaysia in 2016, where his doctoral research focused on advanced digital power electronics and intelligent control systems. From 2016 to 2021, he served as the Director of the Institute for Scientific Publishing and Publications (LPPI) at UAD, where he led initiatives to strengthen research visibility, journal management, and international collaboration in scholarly publishing. Since 2024, he has served as the head of the master's program in electrical engineering at UAD, following his leadership of the undergraduate program in electrical engineering in 2022. He is also the founding leader of the Embedded Systems and Power Electronics Research Group (ESPERG), which actively collaborates with both national and international institutions on topics such as fault-tolerant embedded systems, FPGA-based control, and renewable energy integration. He is widely acknowledged for his contributions to digital design, industrial electronics, motor drives, robotics, intelligent systems, and AI-based automation. His interdisciplinary research emphasizes practical deployments in industrial and healthcare contexts, covering FPGA applications, embedded systems, power electronics, and digital libraries. He has published 380 peer-reviewed articles in high-impact journals and conferences indexed by Scopus. As of 2025, Google Scholar indicates over 6,000 citations, with an h-index of 36 and an i10-index of 174. In recognition of his global research impact, he has been listed among the Top 2% of Scientists Worldwide by Stanford University and Elsevier BV from 2021 to the present, a distinction based on standardized citation metrics across all scientific disciplines. He can be contacted at email: tole@te.uad.ac.id.